Lattice dynamics and thermal properties of $CaWO_4$

A. Senyshyn*
Institute for Materials Science, Darmstadt University of Technology, Petersenstrasse 23, Darmstadt D-64287, Germany

H. Kraus and V. B. Mikhailik
Department of Physics, University of Oxford, Keble Road, Oxford OX1 3RH, United Kingdom

V. Yakovyna
Lviv Polytechnic National University, 12 Bandera St, Lviv 79013, Ukraine
(Received 27 August 2004; published 23 December 2004)

Thermodynamic properties of $CaWO_4$ were studied using the GULP code incorporating semiclassical simulations based on quasiharmonic lattice dynamics and static lattice minimisation methods. Free energy minimization along with so called "relax" fitting was used to obtain the parameters characterising the interatomic interaction potential. From analyses of the calculated and experimental cell sizes, thermal expansion coefficients, elastic constants, phonon density of states, heat capacity, entropy, and Grüneisen parameters it is concluded that quasiharmonic lattice dynamics give a good description of these properties of $CaWO_4$ at temperatures up to 800 K.

DOI: 10.1103/PhysRevB.70.214306 PACS number(s): 63.70.+h, 65.40.De, 65.40.Ba

I. INTRODUCTION

Recent progress achieved in the field of low-temperature detection techniques has lead to the development of highly sensitive energy resolving cryogenic detectors. These devices, when operating in a calorimetric mode, are capable of detecting the energy deposited in their absorbers after particle or radiation interaction. It is the very high resolving power of cryogenic detectors that makes them interesting for an increasing number of applications in fundamental[1–3] and applied sciences.[4–6]

Further advances in the development of cryogenic detectors for rare event search in particle physics rely on the implementation of an event type discrimination technique for detection of radiation and particles. Different types of interaction events, causing electron and nuclear recoils, can be identified by simultaneous measurement of a combination of phonon and scintillation signals from detectors operating at temperatures in milli-K range.[7,8] This technique provides the unique advantage of discrimination against backgrounds that is crucially important for rare-events searches and low-background physics experiments: in particular in the search for weakly interacting massive particles (WIMP's), the preferred candidate for dark matter. Consequently, the next generation of "hybrid" cryogenic phonon-scintillation detectors designated for dark matter experiments is being constructed.[9,10] Calcium tungstate scintillators are considered to be most suitable target materials for such detectors, offering excellent discrimination between nuclear and electron recoils and an energy threshold $\leqslant 3$ keV.[11]

The use of $CaWO_4$ in cryogenic searches for dark matter created a need of knowing the fundamental physical characteristics of this material over a wide temperature range. There exists a significant legacy of research work on calcium tungstate; for example, studies of crystal structure,[12,13] investigations of thermal properties,[14–16] elastic constants,[17–19] phonon dispersion,[20] neutron scattering,[21] IR and Raman spectra,[22,23] studies of scintillation[24] and luminescence properties,[25–28] and electronic structure calculations[29] have been carried out by several groups. Obviously these studies form a solid background for our understanding of the major physical properties of the material of interest. Nonetheless the objective of optimizing the target material for use in cryogenic phonon-scintillation detectors requires a comprehensive characterization of calcium tungstate. In particular the optical and phonon properties of $CaWO_4$ at low temperatures are of high interest, given the features of the "hybrid" detection technique. While extensive studies of the luminescence properties are being actively conducted[30–34] there is still a lack of pertinent investigations of the phonon properties of the crystal. Earlier studies of the lattice dynamics (LD) of $CaWO_4$ using a self-consistent approach,[20,21] implied fitting a model of interatomic interactions using several phonon frequencies and subsequent calculation of the phonon spectrum of the crystal. Such a formalism imposes obvious limitations regarding successful application to the interpretation of the entire set of the physical properties, i.e., elastic, thermal, and optical parameters associated with the LD of the crystal.

Bearing in mind the importance of such information for material science in general and for cryogenic detectors in particular we carried out theoretical modeling of the LD of calcium tungstate based on the quasiharmonic approximation and static lattice energy minimization routine. In this paper we present a model of interatomic interactions that we used to describe the physical properties of $CaWO_4$ in that temperature region. Complex simulations of thermal properties of the crystals in the low- and intermediate-temperature region are performed in order to test the validity of the model.

II. CRYSTAL STRUCTURE

$CaWO_4$ has a sheelite-type structure characterized by a body centered tetragonal space group $I4_1/a$ with four mol-

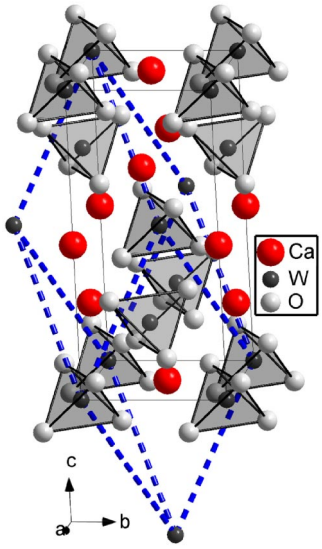

FIG. 1. (Color online) Structure of $CaWO_4$. Solid and dashed lines show the tetragonal and primitive cell, respectively.

ecules per unit cell.[12,13] The result of neutron diffraction from single-crystalline $CaWO_4$ reported by Kay *et al.* (Ref. 12) provides the following lattice parameters for $CaWO_4$: $a=5.243(2)$ Å and $c=11.376(3)$ Å. Figure 1 shows the atom positions in the unit cell of the crystal. Four oxygen atoms are arranged around the tungsten in an isolated tetrahedron, which is compressed along the c axis by 7% over a regular tetrahedron. It should be noted that the presence of the isolated WO_4 tetrahedra is a distinctive feature of the sheelite structure that substantiates the use of a quasimolecular anion complex approximation for the interpretation of the physical properties of the crystal. Each Ca cation shares corners with eight adjacent WO_4 tetrahedra. The bond between the Ca^{2+} cation and WO_4^{2-} anion is mainly ionic, whereas inside the WO_4 complex the W—O bonds are primarily covalent.

It should be noted that the tetragonal cell represents a particular case of the more general primitive cell-rhombohedra with the following parameters: a_p, b_p, c_p, $\alpha_p = \beta_p \neq \gamma_p$. The relationships between the parameters of a tetragonal and a rhombohedral primitive cell are determined by the formulas

$$a_p = \frac{1}{2}\sqrt{2a^2 + c^2}, \quad \alpha_p = \arccos\left(\frac{-c^2}{2a^2 + c^2}\right),$$

$$\gamma_p = \arccos\left(\frac{-2a^2 + c^2}{2a^2 + c^2}\right), \tag{1}$$

where a and c are the parameters of the tetragonal lattice. In our opinion the use of the primitive cell is justified when analyzing the structural changes, e.g., pressure induced sheelite-wolframite phase transitions.[23,35]

III. COMPUTATIONAL METHODOLOGY

The parameters of interatomic interactions were computed and successfully refined by fitting experimental structural data[12] and elastic constants of $CaWO_4$ (Refs. 17 and 19) to a theoretical model, based on a static lattice minimization procedure implemented in the GULP code.[36]

The dominant contribution to the interactions potentials in the crystal results from the Coulomb interaction, which contains more than 90% of the crystal energy. The canonical expression for the Coulomb interaction potential is as follows:

$$U_{ij}^{\mathrm{Coul}}(r_{ij}) = \frac{Z_i Z_j e^2}{r_{ij}}, \tag{2}$$

where Z_i denotes an effective charge of the ith atom while r_{ij} stands for the distance between atoms i and j. Long-range Coulomb interactions were averaged using the Ewald summation, being an optimal approach for simulation of computational clusters with a number of particles less than 10^4. The effective charge of tungsten (Z_W) serves as a fitting parameter for modelling the covalence effect of W-O bonds. In the course of fitting the variation of the effective charge of Ca was found to be very small and therefore was chosen to be fixed as $Z_{Ca}=+2$. Finally, the requirement of charge neutrality yields an effective charge for oxygen: $Z_O=-0.25(Z_{Ca}+Z_W)$. For modelling the atomic interaction the linear combination of Coulumb and repulsion potential was chosen. The repulsion potential for Ca-O interaction was modelled as a linear combination of Born-Mayer and van der Waals energies (so called Buckingham potential), which is typically used for simulations of ionic compounds and bonds

$$U_{ij}^{\mathrm{Buck}}(r_{ij}) = b_{ij}\exp\left(-\frac{r_{ij}}{\rho_{ij}}\right) - \frac{c_{ij}}{r_{ij}^6}, \tag{3}$$

where the first and second terms represent the Born-Mayer and van der Waals energies, respectively, b_{ij}, ρ_{ij}, and c_{ij} are the potential parameters for each pair of atoms. For modeling the O-O interaction the Buckingham potential from the paper of Gavezzotti[37] was used.

To describe the repulsion in the W-O interactions the analytical form of the Morse potential was applied, which is typically used in simulations of covalent compounds and bonds

$$U_{ij}^{\mathrm{Morse}}(r_{ij}) = D(\{1 - \exp[-a_m(r - r_0^2)]\} - 1). \tag{4}$$

Here D, a_m, and r_0 are the parameters of the Morse potential and D represents the bond energy and r_0 is the sum of the bond radii. The cutoff for pairwise short-range interactions is selected to be equal $\sim 2a_p$, where a_p is the primitive cell parameter.

For modeling the WO_4 tetrahedra the harmonic three-body potential was chosen as

$$U_{ijk}^{\mathrm{three}}(\theta) = \frac{1}{2}k_{\mathrm{three}}(\theta - \theta_0)^2, \tag{5}$$

where θ is the angle between atoms i, j, and k and k_{three} is a force constant. The equilibrium angle θ_0 was obtained from an analysis of the $CaWO_4$ structure as being equal to 110.5° (1.929 rad).

TABLE I. Parameters of interatomic interaction potential.

Coulomb potential [Eq. (2)]			
Atoms		Z_i, e	
Ca		2.0	
W		1.807189	
O		−0.9282305	
Buckingham potential [Eq. (3)]			
Pair of atoms	b, eV	ρ, Å	c, eV Å^6
Ca-O	2312.0	0.2812	0.0
O-O	2023.8	0.2674	13.83
Morse potential [Eq. (4)]			
Pair of atoms	D, eV	a_m, Å^{-2}	r_0, Å
W-O	1.501	2.671	1.8928
Three-body potential [Eq. (5)]			
Three-body	k_{three}, eV rad^{-2}	θ_0, rad	
O-W-O	2.6071	1.929	

IV. RESULTS AND DISCUSSION

A. Parameters of the interatomic interaction potential

Having now constructed the model of interatomic interactions, the experimental structure parameters and four elastic constants[38] at temperature 300 K and pressure 1 atm were fitted simultaneously using the GULP (General Utility Lattice Program) code using the free energy minimization and "relax" fitting techniques.[39] The best agreement between calculated and experimental properties was obtained with the parameters of the interatomic interaction potential listed in Table I.

For this set of interaction parameters one notices an encouraging agreement between the experimental and calculated lattice parameters (Table II). The calculated elastic constants were found to fit the experimental values with ~10% accuracy which is entirely acceptable for semiclassical calculations. Thus, the use of quasiharmonic LD and the self-consistent approach indeed yields a reasonable agreement between the experimental and calculated characteristics of $CaWO_4$. Bearing in mind that this approach has already proved to be appropriate for modelling of thermodynamic characteristics of solids over a wide temperature range,[40,41] this finding justifies the use of the technique for modelling the changes with temperature of the $CaWO_4$ properties.

Using the above model of interatomic interactions and free energy minimization technique we carried out simulations of structural properties of $CaWO_4$ in the temperature range 0–1250 K. The calculated thermal changes of the lattice parameters are shown in Fig. 2 as filled symbols together with the experimental results of Deshpande and Suryanarayana[42] (open symbols). The dashed curves in Fig. 2 represent a fit of the calculated lattice parameters to a function of temperature:

TABLE II. Experimental and calculated properties of $CaWO_4$ at $T=300$ K and $P=1$ atm.

Properties		Experiment		Calculation
Structural parameters				
a, Å		5.243(2)		5.2435
c, Å		11.376(3)		11.3740
V, Å^3		312.7		312.72
Ca	$x/a, y/b, z/c$	0,0,1/2		0,0,1/2
W	$x/a, y/b, z/c$	0,0,0		0,0,0
O	x/a	0.2413(5)		0.2435
	y/b	0.1511(6)		0.1504
	z/c	0.0861(1)		0.0846
Elastic constants[a]				
$\boldsymbol{C_{11}}$, GPa		143.870	145.9	145.06
$\boldsymbol{C_{33}}$, GPa		130.180	127.4	121.84
$\boldsymbol{C_{12}}$, GPa		63.501	62.6	60.90
C_{13}, GPa		56.170	39.2	40.28
C_{16}, GPa		−16.355	−19.2	−11.91
$\boldsymbol{C_{44}}$, GPa		33.609	33.5	38.83
C_{66}, GPa		45.073	38.7	52.68

[a]The first and second columns of data in the experimental "elastic constants" subsection are experimental data of Gluyas *et al.* (Ref. 17) and Farley and Saunders (Ref. 19), respectively. Only averaged C_{11}, C_{12}, C_{33}, and C_{44} elastic constants (shown in bold) were used in our calculation of interatomic interactions.

$$F(T) = a_0[1 + a_1T^2 + a_2T^3 + a_3T^4], \tag{6}$$

where a_0, a_1, a_2, a_3 are fitting coefficients summarized in Table III.

It should be noted that the data presented in Fig. 2 demonstrate good agreement between experimental and calculated lattice parameters. Nonetheless the lack of experimental results particularly in the low-temperature range invokes the necessity of additional structural investigations of $CaWO_4$ over a wide temperature range.

B. Thermal expansion coefficients

The thermal expansion coefficient (TEC) can be derived from the lattice parameters (l) and cell volume as follows:

$$\alpha_l = \frac{\partial \ln(l)}{\partial T}. \tag{7}$$

Let us consider the thermal behavior of anisotropic and volumetric TEC's calculated from the thermal dependences of lattice parameters and cell volumes which, in turn, were obtained using GULP (solid points in Fig. 2)

The results of numerical differentiation of the calculated cell parameters via Eq. (7) are presented in Fig. 3 as solid symbols. Solid curves in Fig. 3 show TEC's obtained from interferometric measurements of Yates and Bailey,[15] dashed

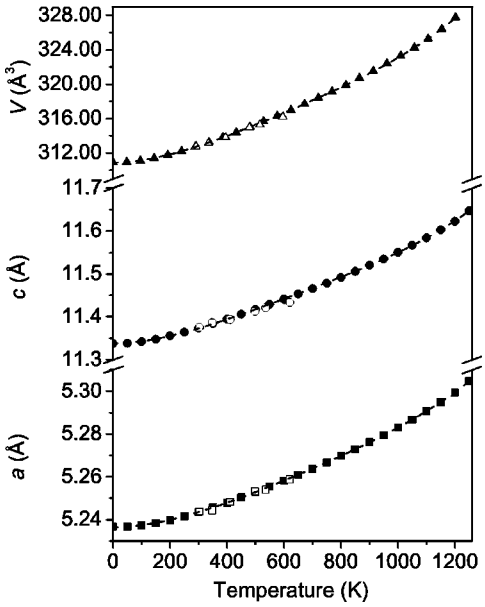

FIG. 2. Thermal dependences of lattice parameters and cell volume. Open symbols—experimental results of Deshpande and Suryanarayana (Ref. 42), solid symbols—results of calculations in this paper.

curves represent TEC's reported by Deshpande and Suryanarayana,[42] and finally horizontal doted lines show values of TEC's for four selected temperature intervals (as given in the paper of Nassau and Hroyer,[43] who measured the expansion of $CaWO_4$ using a quartz dilatometer in the temperature range 77–1298 K). For crystals with tetragonal symmetry the volumetric TEC α_V is equal $\alpha_V=2\alpha_a+\alpha_c$, where α_a and α_c denotes TEC in the a and c directions, respectively. We calculated α_V by differentiation of the temperature dependence of the cell volumes while the "reference" one was obtained by summation of the respective anisotropic TEC's from the literature cited.

It is clear that the calculated temperature dependences of the TEC's show fairly good agreement with the results of Yates and Bailey[15] measured at low temperatures ($T \leqslant 300$ K) and reasonable agreement with the experimental data in the 300–800 K temperature range. However at $T \geqslant 800$ K the TECs exhibit a pronounced increase and anomalously high values. This artifact is likely due to an inherent constraint of the quasiharmonic approximation that impedes adequate simulation of the $CaWO_4$ TEC's in the high-temperature region.

TABLE III. The results of a polynomial fit of the lattice parameters to Eq. (6).

	Lattice parameter a	Lattice parameter c
a_0	5.23643±0.00005	11.33815±0.00033
$a_1\times10^8$	1.9552±0.0178	4.5968±0.0526
$a_2\times10^{11}$	−1.7391±0.0339	−4.5121±0.0999
$a_3\times10^{14}$	0.6732±0.0166	1.7828±0.0489
R (COD)	0.99998	0.99995

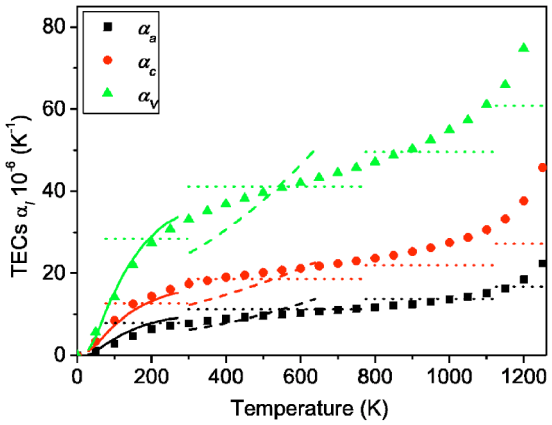

FIG. 3. (Color online) Calculated (symbols) and measured thermal expansion coefficient of $CaWO_4$ as functions of temperature. Solid curves show data of Yates and Bailey (Ref. 15); dashed curves, data of Deshpande and Suryanarayana (Ref. 42); and horizontal dotted lines, values of TEC's for four selected temperature intervals according to Nassau and Hroyer (Ref. 43).

C. Elastic and phonon properties

According to the Grüneisen law[44] the volumetric TEC can be expressed via the Grüneisen parameter γ_V, density of the material ρ, isothermal or adiabatic bulk moduli K_T and K_S, and the heat capacities at constant volume and pressure C_V and C_P using the following expression:

$$\alpha_V = \frac{\gamma_V \rho C_V}{K_T} = \frac{\gamma_V \rho C_P}{K_S}. \tag{8}$$

Our intention is to consider the parameters of Eq. (8) in detail. First, let us analyze the elastic properties of calcium tungstate. Elastic constants were calculated as second derivatives of the energy density with regard to external strain. The elastic moduli were obtained using the Reuss-Voight-Hill averaging scheme for the tensor of elastic constants.[45] The calculated elastic moduli are presented in Fig. 4 by solid symbols along with "experimental" ones, i.e., obtained from the

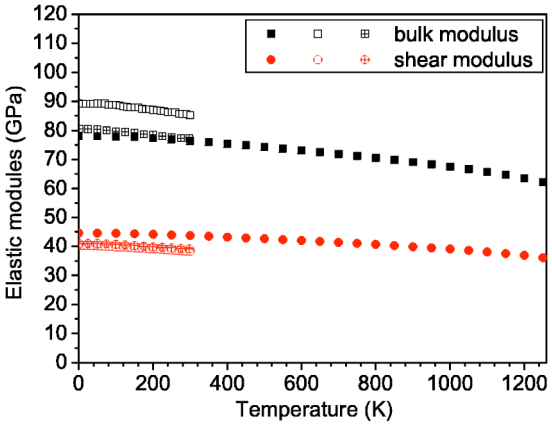

FIG. 4. (Color online) Calculated (solid symbols) and measured elastic moduli of $CaWO_4$ as functions of temperature. Open symbols are data received from the measurements of Glyuas *et al.* (Ref. 17), crossed symbols from Farley and Saunders (Ref. 19).

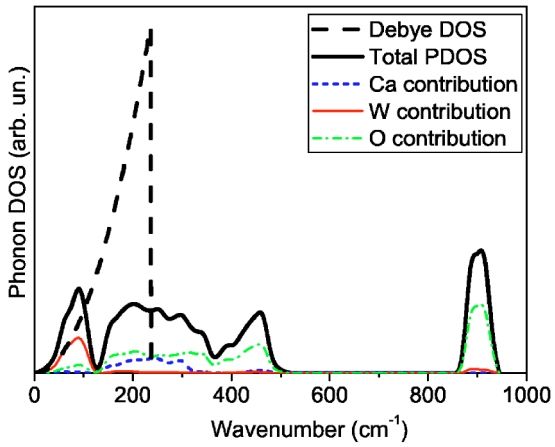

FIG. 5. (Color online) The phonon density of states at 300 K and 1 atm. The areas occupied by Debye DOS and total PDOS were selected to be equal.

averaging of measured elastic constants from Ref. 17 (open symbols) and Ref. 19 (crossed symbols). Figure 4 demonstrates reasonable agreement between the "experimental" and calculated bulk K and shear G moduli. It is apparent that the calculated temperature dependence of the bulk modulus is much closer to that derived from the data of Farley and Saunders.[19] Finally it needs to be noted that the value of a bulk modulus at room temperature ($K=77\pm8$ GPa), which has recently been obtained from the pressure dependence of a cell volume of a $CaWO_4$ sheelite crystal[35] by fitting to the third-order Birch-Murnaghan equation of state, agrees very well with the calculated one.

Next, we performed analysis of the LD properties of the crystals. The phonon spectrum was calculated using constructed interatomic interaction potentials with parameters listed in Table I and the Born-von Karman equations of LD incorporated into the GULP code.[36] The phonon density of states (PDOS) was obtained by integration of the Brillouin zone taking into account its symmetry. The Monkhorst-Pack method[46] with a $12\times12\times12$ grid was used for the integration. All calculated branches of the phonon spectrum yield positive frequencies indicating the stability of the potential model. The results of the calculations are presented in Fig. 5 together with the PDOS determined from classic Debye theory:

$$g(\omega)=\begin{cases} 9nZ\left(\dfrac{\hbar}{k_B\theta_D}\right)^2\omega^2, & \omega\leqslant\dfrac{k_B\theta_D}{\hbar}, \\ 0, & \omega>\dfrac{k_B\theta_D}{\hbar}, \end{cases} \qquad (9)$$

where ω is the frequency, θ_D is the Debye temperature, which is taken as being equal to 355 K,[47] $\hbar$ and k_B are Planck and Boltzmann constants, respectively, n is the number of atoms in formula unit, and Z is the number of formula units in the cell.

As can be seen from Fig. 5, at frequencies above ~30 cm^{-1} the shape of the calculated PDOS differs significantly from the parabolic law of dispersion postulated by Debye theory. Hence, similarly to other oxide compounds, e.g., $MgSiO_3$ (Ref. 40) and $Nd_{0.75}Sm_{0.25}GaO_3$ (Ref. 41), $CaWO_4$ is not a good Debye-like solid, which may be reflected in pronounced differences between thermodynamic properties calculated from the phonon spectrum and in the framework of Debye theory.

With the constructed interatomic interaction potential, it appears to be possible to simulate the band gap in the phonon spectrum between low-frequency lattice modes and high-frequency internal modes of WO_4 tetrahedra, as is reported in the literature.[23,48,49] For additional demonstration we calculated the projections of the atomic contributions to the total PDOS. An analysis of the contributions of the calcium, tungsten and oxygen atoms to the total PDOS, presented in Fig. 5 shows that calcium gives a noticeable contribution to the lattice modes only, whereas tungsten, owing to its heavy mass, dominates in the low-frequency part of the lattice mode region and participates in the internal modes of the WO_4 tetrahedra. Accordingly, oxygen atoms contribute to both lattice and internal modes.

The deviation of the calculated PDOS from the experimental one could be determined by comparing the experimental and calculated integral characteristics of the phonon spectrum, i.e., thermodynamic properties (heat capacity at constant volume C_V and entropy S) which can be easily obtained from the total PDOS using the following relations:

$$C_V(T)=k_B\int_0^{\omega_{\max}}g(\omega)\left(\frac{\hbar\omega}{k_BT}\right)^2\frac{\exp\left(\dfrac{\hbar\omega}{k_BT}\right)}{\left[\exp\left(\dfrac{\hbar\omega}{k_BT}\right)-1\right]^2}d\omega,$$

$$S(T)=\int_0^{\omega_{\max}}g(\omega)\left\{\frac{1}{T}\frac{\hbar\omega}{\exp\left(\dfrac{\hbar\omega}{k_BT}\right)-1}-k_B\times\ln\left[1-\exp\left(-\frac{\hbar\omega}{k_BT}\right)\right]\right\}d\omega, \qquad (10)$$

where $\omega_{\max}$ is the maximal frequency of the phonons. Calculated in this way thermodynamic properties are presented in Figs. 6(a) and 6(b) as solid squares. To obtain a pertinent relationship within the Debye model [dashed curves in Figs. 6(a) and 6(b)], the Debye PDOS calculated from Eq. (9) was used as input parameter $g(\omega)$ for Eq. (10). The results of these computations are shown in Fig. 6 together with the data of calorimetric measurements of Lyon and Westrum.[14]

Analysis of the results presented in Figs. 6(a) and 6(b) allows one to draw the conclusion that the Debye theory describes satisfactorily the thermodynamic properties of $CaWO_4$ only for temperatures $T\leqslant\theta_D/10$. With increasing temperature the differences between experimental results and data derived from Debye theory become significant because optical phonons play an increasingly important role. It is of interest to note that this conclusion is supported by observation of nonlinear effects in the elastic scattering of THz

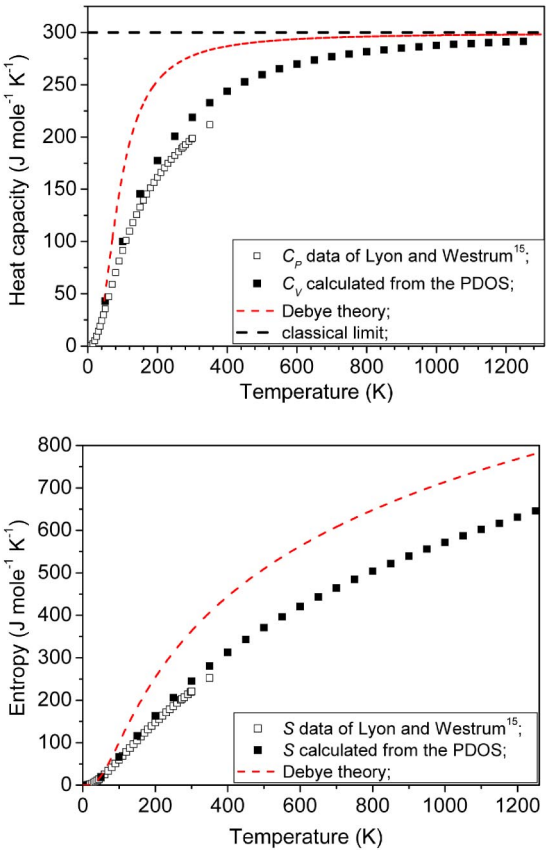

FIG. 6. (Color online) Calculated (solid symbols) and experimental (open symbols) thermodynamic properties of $CaWO_4$ (per primitive cell $Z=2$). Top—heat capacity C_V, bottom—entropy S. Dashed curves show the results of calculations performed within the Debye theory.

phonons (anomalous mode) in $CaWO_4$ using heat pulses at 30–40 K that is associated with the dispersion curves populated at high temperature.[50]

Good agreement on thermodynamic properties is observed for our model over a much wider temperature range (0–150 K), although at higher temperatures one can notice differences between experimental and calculated parameters. Presumably, these differences could be associated with a deviation of the calculated PDOS from the real one. For entropy such deviation was found to be equal ~12% at $T=350$ K. The difference between experimental C_P and calculated C_V is ~9.5%. Taking into account that C_P is usually greater than C_V, this difference is stated to be an underestimate and one should adopt ~12%.

D. Debye temperature

Although Debye theory does not provide an adequate description of the phonon spectrum of calcium tungstate the Debye temperature θ_D remains an important characteristic of the material. In the literature two approaches for determination of the Debye temperature are widely used. Firstly, there is the fitting of experimental properties of materials using the Debye-like interpolation formulas. Secondly, θ_D can be calculated from sound velocities (elastic moduli) using the Robie and Edwards equation[51]

$$\theta_D = \frac{\hbar}{k_B}\left(\frac{6\pi^2 nZ}{V}\right)^{1/3}\left[\frac{1}{3}\left(\frac{3K+4G}{3\rho}\right)^{-3/2}+\frac{2}{3}\left(\frac{G}{\rho}\right)^{-3/2}\right]^{-1/3}. \tag{11}$$

For the calculation of the temperature dependence of the Debye temperature a range of different authors used fitting of the heat capacity to respective Debye functions (Refs. 14, 15, and 17). However, as was already pointed out, the Debye theory describes thermodynamic properties of $CaWO_4$ only at low temperatures ($T \leqslant \theta_D/10$), where acoustic phonons play the dominant role. Therefore fitting to thermodynamic functions at higher temperatures is inadequate due to the impossibility of appropriate elimination of the contributions caused by optical phonons. Furthermore, in the course of calculating the Debye temperatures, these authors considered calcium tungstate as a diatomic solid composed of Ca^{2+} cations and $(WO_4)^{2-}$ anion complexes that results in an underestimation of the Debye temperature. Yates and Bailey[15] analyzed experimental results of Lyon and Westrum[14] and determined θ_D from the limiting slope of the heat capacity against T^3 as 267±15 K using the low-temperature relation

$$C_V(T) = \frac{12}{5}\pi^4 nZR\left(\frac{T}{\theta_D}\right)^3, \tag{12}$$

where R denotes the universal gas constant.

Gluyas *et al.*[17] obtained a Debye temperature of 246.5 K from elastic constants using an expression similar to Eq. (11). In the calculations of both groups, $n=2$ was assumed as for a diatomic solid, when the number of atoms in the formula unit should be 6. As a matter of fact the WO_4 tetrahedron does exhibit a pronounced chemical stability in $CaWO_4$ but in our opinion this has no relation to the dynamics of phonons in this compound and there are no firm reasons to make such a simplification that causes a $\sqrt[3]{3}$ times underestimate of θ_D. When taking this reasoning into account the recalculated values of θ_D should be as given in Table IV.

In order to clarify this disputable issue, the Debye temperatures were determined using several different approaches. First we analyzed the calculated low-temperature heat capacity and entropy expressed as C_V/T^3 and S/T^3 as function of T in the 0–30 K temperature range in 1 K steps. The respective Debye temperatures were determined from the low-temperature plateaus of the plots. Next, the value of θ_D was derived using the experimental elastic constants of $CaWO_4$ measured by Farley and Saunders[19] and by Glyuas *et al.*[17] near $T=0$ *K*. Finally, the value of θ_D was obtained using the elastic moduli calculated by us. Debye temperatures calculated using the different methods are presented in the Table IV. Inspecting these results one can see that for the value of θ_D reported by Yates and Bailey[15] there is no sufficient statistics, which caused significant error. As for the Debye temperature obtained from the calculated elastic moduli it should be noted that due to an ~10% overestimate of the calculated shear modulus compared with the experimental results of Farley and Saunders[19] and Glyuas *et al.*[17] (see Fig. 4) the respective Debye temperature is ~20 K higher. With

TABLE IV. Isothermal Debye temperatures of $CaWO_4$.

Method of determining	Reference	Debye temperature, K
Slope C_P [Lyon and Westrum (Ref. 14)] vs T^3	Yates and Bailey (Ref. 15)	385 ± 25[a]
Elastic moduli (Ref. 17)	Glyuas *et al.* (Ref. 17)	356[a]
Low-temperature plateau C_V/T^3 (calculated) vs T	This work	351 ± 19
Low-temperature plateau S/T^3 (calculated) vs T	This work	356 ± 20
Elastic moduli (Ref. 17)	This work	354
Elastic moduli (Ref. 19)	This work	357
Elastic moduli (calculated)	This work	379

[a]Recalculated from the respective reference data.

regards to other results summarized in Table IV there is encouraging agreement. Given this, the first and last numbers were excluded from further consideration and the averaged isothermal Debye temperature was found to be 355 K. Accordingly, the PDOS curves (Fig. 5) as well as temperature dependences of C_V and S (Fig. 6) were calculated using standard relations of Debye theory with $\theta_D=355$ *K*.

With regard to this value it is worthwhile noting the results of a recent estimate of the Debye temperature using the luminescence technique. Mikhailik *et al.*[31] investigated thermal changes of the luminescence spectra in the temperature range 8–300 K. To explain the observed temperature shift of the $CaWO_4$ luminescence band, a model of the luminescence centre in a vibrating crystalline environment that use a Debye distribution for the phonon density of states[52] was applied and a value of $\theta_D=300\pm80$ K was obtained. Though the overall precision of this method is assessed to be poor, the derived numerical parameter agrees with the Debye temperature of $CaWO_4$ derived in the present study taking into account the error on the result.

E. Grüneisen parameter

Let us finally consider the Grüneisen parameter. In this study the Grüneisen parameter γ_V was determined from Eq. (8) using α_V, K_T, and C_V obtained in the course of our simulations. The anisotropic Grüneisen parameter (Grüneisen parameter tensor components) γ_a and γ_c were calculated using the methodology of Refs. 15 and 19. Figure 7 presents the Grüneisen parameter calculated in this way. Farley and Saunders[19] reported a thermal dependence of the Grüneisen parameter tensor components. Later Glyuyas *et al.*[17] carried out similar calculations. The results of these calculations are presented in Fig. 7 using solid and dashed curves, respectively. The bold curve in Fig. 7 shows γ_V calculated from Eq. (8) using experimental parameters α_V, K, and C_P measured by Yates and Bailey,[15] Farley and Saunders,[19] and Lyon and Westrum,[14] respectively. As is seen in Fig. 7 Glyuyas *et al.*[17] obtained values of γ_a and γ_c about 10% higher than Farley and Saunders.[19] Taking into account the fact that these authors used the same reference heat capacity[14] and TEC's,[15] this discrepancy can be attributed to the difference in the measured elastic constants. Our calculations yield lower Grüneisen parameters (~15% as obtained from the analysis of the calculated and experimental γ_V), which is presumably the result of an overall discrepancy between calculated and experimental heat capacities, elastic constants and TEC's.

V. CONCLUSION

In this study the LD and thermodynamic properties of crystalline calcium tungstate have been investigated using semiclassical simulations based on quasiharmonic lattice dynamics and a self-consistent static lattice minimization method. A rigid-ion model of classical interatomic interaction was constructed that considers the interatomic interaction potential as a linear combination of Coulomb and Buckingham potentials. In addition, to take into account the effect of covalence inside the WO_4 tetrahedra the partial charges of ions were used and the interaction was simulated using a linear combination of Coulomb and Morse potentials. To emphasise the role of WO_4 tetrahedra a three-body potential about the tungsten ion was applied. Free energy minimization along with the so-called "relax" fitting technique was used to obtain the potential parameters. The approach applied was found to yield results that describe well physical properties of the crystal; an encouraging agreement between the experimental and calculated structural properties and

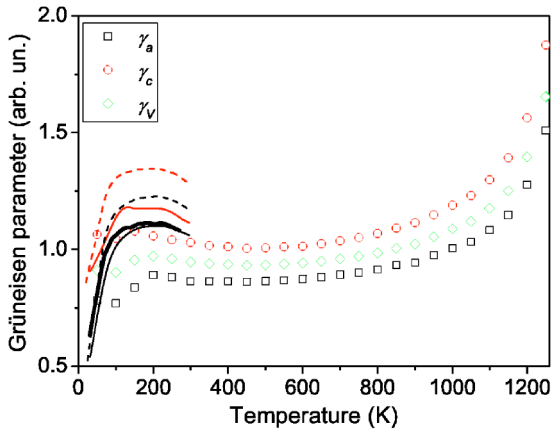

FIG. 7. (Color online) Temperature dependence of the Grüneisen parameters of $CaWO_4$. Solid curves present results of Farley and Saunders (Ref. 19); dotted curves, Glyuyas *et al.* (Ref. 17); and the bold curve, volumetric Grüneisen parameters γ_V calculated from experimental results. Open symbols show results of the computation in this work.

elastic constants was attained. Reassured by this finding we carried out investigations of LD and thermodynamics properties of $CaWO_4$. This included simulation of the thermal evolutions of cell parameters a and c, elastic moduli K and G, heat capacity C_V, entropy S, thermal expansion and Grüneisen tensor components, as well as computation of the PDOS. The temperature behavior of C_P and S together with PDOS were calculated also in the framework of the classical Debye theory. Comparison of these results with the experimental dependences $C_P=f(T)$ and $S=f(T)$ revealed significant differences between experiment and prediction of the Debye model at $T\geqslant 30$ K evidencing that $CaWO_4$ cannot be considered as a good Debye-like solid.

On the other hand the results on temperature dependences of the heat capacity and entropy derived within the quasiharmonic LD models agree very well with the experimental data over a wide temperature range (0–150 K); moreover even at room temperature the resulting discrepancy is ~10% which is presumably the result of overestimating the rigidity of the W-O bonds. Comparison of the cited and calculated properties showed that it is possible to simulate the thermal expansion of $CaWO_4$ and its anisotropy, though precise structural investigations over a wide temperature region are necessary to reconcile the discrepancy between the results of different experimental studies. Reasonable absolute values and thermal dependences are calculated for the elastic moduli of the crystal. Noticeably, the value for the bulk modulus K is coinsistent within the error with that obtained experimentally at room temperature. The calculated Grüneisen parameter γ is found to be ~15% lower than measured in experimental studies. It is pointed out that such a difference can be due to an overall discrepancy between characteristic parameters of $CaWO_4$ that are used to derive γ from the experimental results. Finally, since the Debye temperature θ_D is an important thermodynamic characteristic of the material we used the quasiharmonic LD model to obtain this value for calcium tungstate. We analyzed the results of different experimental studies and reached the consistent conclusion that a value of $\theta_D=355$ K should be adopted.

Altogether these results show that the quasiharmonic LD approach is viable for the practical case. Of particular merit of this approximation is the possibility of describing the key physical properties and predicting the behavior of the material in a practically important temperature range, i.e., from 0 K to room temperature. Given current growing interest in the application of single crystals as cryogenic detector in the experimental search for rare events and considering the crucial importance of understanding of the thermodynamic characteristics of the material, we expect that the use of such a computation technique can be very beneficial for future developments of the cryogenic detectors.

ACKNOWLEDGMENTS

This work was supported in part by PPARC Grant No. I/S/2001/646. We would like to thank Professor Julian D. Gale for providing the GULP code and Dr. Artem R. Oganov for helpful comments on the manuscript. A. Senyshyn gratefully acknowledges the Deutscher Akademischer Austauschdienst (German Academic Exchange Service) for financial support.

*Electronic address: senyshyn@st.tu-darmstadt.de; Also at: Semiconductor Electronics Department, Lviv Polytechnic National University, 12 Bandera St, Lviv 79013, Ukraine.

[1] M. Bravin, M. Bruckmayer, C. Bucci, S. Cooper, S. Giordano, F. von Feilitzsch, J. Höhne, J. Jochum, V. Jörgens, R. Keeling, H. Kraus, M. Loidl, J. Lush, J. Macallister, J. Marchese, O. Meier, P. Meunier, U. Nagel, T. Nussle, F. Pröbst, Y. Ramachers, H. Sarsa, J. Schnagl, W. Seidel, I. Sergeyev, M. Sisti, L. Stodolsky, S. Uchaikin, and L. Zerle, Astropart. Phys. **12**, 107 (1999).

[2] H. Kraus, Philos. Trans. R. Soc. London, Ser. A **361**, 2581 (2003).

[3] E. Fiorini, Nucl. Instrum. Methods Phys. Res. A **520**, 1 (2004).

[4] H. Kraus, Int. J. Mass. Spectrom. **215**, 45 (2002).

[5] T. Nakamura, M. Katagiri, M. Ukibe, T. Ikeuchi, and M. Ohkubo, Nucl. Instrum. Methods Phys. Res. A **520**, 67 (2004).

[6] P. Christi, S. Rutzinger, C. Koy, W. Seidel, S. Uchaikin, M. O. Glocker, and F. Pröbst, Eur. J. Mass Spectrom. **10**, 469 (2004).

[7] A. Alessandrello, V. Bashkirov, C. Brofferio, C. Bucci, D. V. Camin, O. Cremonesi, E. Fiorini, G. Gervasio, A. Giuliani, A. Nucciotti, M. Pavan, G. Pessina, E. Previtali, and L. Zanotti, Phys. Lett. B **420**, 109 (1998).

[8] P. Meunier, M. Bravin, B. Bruckmayer, S. Giordano, M. Loidi, O. Meier, F. Pröbst, W. Seidel, M. Sisti, L. Stodolsky, S. Uchaikin, and L. Zerle, Appl. Phys. Lett. **75**, 1335 (1999).

[9] G. Angloher, M. Bruckmayer, C. Bucci, M. Bühler, S. Cooper, C. Cozzini, P. Di Stefano, F. V. Feilitzsch, T. Frank, D. Hauff, T. Jagemann, J. Jochum, V. Jorgens, R. Keeling, H. Kraus, M. Loidl, J. Marchese, O. Meier, U. Nagel, F. Pröbst, Y. Ramachers, A. Rulofs, J. Schnagl, W. Seidel, I. Sergeyev, M. Sisti, M. Stark, S. Uchaikin, L. Stodolsky, H. Wulandari, and L. Zerle, Astropart. Phys. **18**, 43 (2002).

[10] S. Cebrian, N. Coron, G. Dambier, E. García, I. G. Irastorza, J. Leblanc, P. de Marcillac, A. Morales, J. Morales, A. Ortiz de Solórzano, J. Puimedon, M. L. Sarsa, and J. A. Villar, Astropart. Phys. **21**, 23 (2004).

[11] G. Angloher, C. Bucci, C. Cozzini, F. von Feilitzsch, T. Frank, D. Hauff, S. Henry, Th. Jagemann, J. Jochum, H. Kraus, B. Majorovits, J. Ninkovic, F. Petricca, F. Pröbst, Y. Ramachers, W. Rau, W. Seidel, M. Stark, S. Uchaikin, L. Stodolsky, and H. Wulandari, Nucl. Instrum. Methods Phys. Res. A **520**, 108 (2004).

[12] M. I. Kay, B. C. Fraizer, and I. J. Almodovar, J. Chem. Phys. **40**, 504 (1964).

[13] R. M. Hazen, L. W. Finger, and J. W. E. Mariathasan, J. Phys. Chem. Solids **46**, 253 (1985).

[14] W. G. Lyon and E. F. Westrum, J. Chem. Phys. **49**, 3374 (1968).

[15] B. Yates and A. C. Bailey, J. Low Temp. Phys. **4**, 117 (1971).

[16] A. A. Khan, Acta Crystallogr., Sect. A: Cryst. Phys., Diffr., Theor.

Gen. Crystallogr. **32**, 11 (1976).
[17] M. Gluyas, F. D. Hughes, and B. W. James, J. Phys. D **6**, 2025 (1973).
[18] J. M. Farley and G. A. Saunders, Solid State Commun. **9**, 965 (1971).
[19] J. M. Farley and G. A. Saunders, J. Phys. C **5**, 3021 (1972).
[20] K. Kesavasamy and N. Krishnamurthy, Can. J. Phys. **60**, 1447 (1982).
[21] D. K. Steinman, J. S. King, and H. G. Smith, (unpublished).
[22] A. S. Barker, Phys. Rev. **135**, A742 (1964).
[23] D. Cristofilos, S. Ves, and G. A. Kourouklis, Phys. Status Solidi B **198**, 539 (1996).
[24] G. B. Beard, W. H. Kelly, and M. L. Mallory, J. Appl. Phys. **33**, 144 (1962).
[25] M. J. Treadaway and R. C. Powel, J. Chem. Phys. **61**, 4003 (1974).
[26] R. Grasser, A. Sharmann, and K.-R. Strack, J. Lumin. **27**, 263 (1982).
[27] G. Blasse and G. Bokkers, J. Solid State Chem. **49**, 126 (1983).
[28] V. V. Mikhailin, A. N. Belsky, I. A. Kamenskikh, V. N. Kolobanov, P. A. Orekhanov, I. N. Shpinkov, D. A. Spassky, and A. N. Vasil'ev, Nucl. Instrum. Methods Phys. Res. A **486**, 367 (2002).
[29] Y. Zhang, N. A. W. Holzwarth, and R. T. Williams, Phys. Rev. B **57**, 12 738 (1998).
[30] V. B. Mikhailik, I. K. Bailiff, H. Kraus, P. A. Rodnyi, and J. Ninkovic, Radiat. Meas. **38**, 585 (2004).
[31] V. B. Mikhailik, H. Kraus, D. Wahl, M. Itoh, M. Koike, and I. K. Bailiff, Phys. Rev. B **69**, 205110 (2004).
[32] V. B. Mikhailik, H. Kraus, G. Miller, M. S. Mykhaylyk, and D. Wahl, (unpublished).
[33] J. Ninkovic, G. Angloher, C. Bucci, C. Cozzini, T. Frank, D. Hauff, H. Kraus, B. Majorovits, V. Mikhailik, F. Petricca, F. Pröbst, Y. Ramachers, W. Rau, W. Seidel, and S. Uchaikin, (unpublished).
[34] V. Yakovyna, A. Matkovskii, D. Sugak, I. Solskii, and S. Novosad, Radiat. Meas. **38**, 403 (2004).
[35] D. Errandonea, M. Somayazulu, and D. Häusermann, Phys. Status Solidi B **235**, 162 (2003).
[36] J. D. Gale, Philos. Mag. B **73**, 3 (1996).
[37] A. Gavezzotti, Acc. Chem. Res. **27**, 309 (1994).
[38] Actually the deformation of the tetragonal cell is described by seven elastic constants C_{11}, C_{33}, C_{12}, C_{13}, C_{16}, C_{44}, C_{66}. The elastic constant tensor of calcium tungstate was studied independently by Gluyas *et al.* (Ref. 17) and Farley and Saunders (Ref. 19) by measuring ultrasound wave velocities. A comparison of the results of these authors shows that the difference between experimental elastic constants C_{11}, C_{12}, C_{33}, and C_{44} is not greater than 2.5%, whereas for elastic constants C_{13}, C_{16}, C_{66} a pronounced discrepancy ($\geqslant 15\%$) is observed (see Table II). Therefore only averaged C_{11}, C_{12}, C_{33}, and C_{44} elastic constants were used in our modeling of interatomic interactions.
[39] J. D. Gale and A. L. Rohl, Mol. Simul. **29**, 291 (2003).
[40] A. R. Oganov, J. P. Brodholt, and G. D. Price, Phys. Earth Planet. Inter. **122**, 277 (2000).
[41] A. Senyshyn, A. R. Oganov, L. Vasylechko, H. Ehrenberg, U. Bismayer, M. Berkowski, and A. Matkovskii, J. Phys.: Condens. Matter **16**, 253 (2004).
[42] V. T. Deshpande and S. V. Suryanarayana, J. Mater. Sci. **7**, 255 (1972).
[43] K. Nassau and A. M. Hroyer, J. Appl. Phys. **33**, 3064 (1962).
[44] O. L. Anderson, Am. Mineral. **83**, 23 (1998).
[45] B. P. Belikov, K. S. Aleksandrov, and T. V. Ryzhova, *Elastic Constants of Rock-Forming Minerals* (Nauka, Moscow, 1970) (in Russian).
[46] H. J. Monkhorst and J. D. Pack, Phys. Rev. B **13**, 5 188 (1976).
[47] For a discussion on the value of the Debye temperature used in these computations see Sec. IV D.
[48] A. Jayaraman, B. Batlogg, and L. G. VanUitert, Phys. Rev. B **28**, 4774 (1983).
[49] J. Hanuza, K. Hermanovicz, W. Ryba-Romanowski, H. Drulis, and E. I. Uspensky, Pol. J. Chem. **68**, 185 (1994).
[50] J. K. Wigmore, A. G. Kozorezov, Hamid bin Rani, M. Giltrow, H. Kraus, and B. M. Taele, Physica B **316–317**, 589 (2002).
[51] R. A. Robie and J. L. Edwards, J. Appl. Phys. **37**, 2659 (1966).
[52] B. Henderson and G. F. Imbusch, *Optical Spectroscopy of Inorganic Solids* (Clarendon Press, Oxford, 1989).